Programa de Pós-Graduação em Ciência dos Materiais[1]; Programa de Pós-Graduação em Ciências Farmacêuticas[2], Faculdade de Farmácia; Departamento de Química Orgânica[3], Instituto de Química, Universidade Federal do Rio Grande do Sul, Brasil

Solid lipid nanoparticles containing copaiba oil and allantoin: development and role of nanoencapsulation on the antifungal activity

G. Svetlichny[1], I. C. Külkamp-Guerreiro[2], S. L. Cunha[2], F. E. K. Silva[2], K. Bueno[2], A. R. Pohlmann[2], A. M. Fuentefria[2], S. S. Guterres[1,2]

Received August 1, 2014, accepted October 5, 2014

Prof. Silvia Guterres, Programa de Pós-Graduação em Ciências Farmacêuticas, Universidade Federal do Rio Grande do Sul, Av. Ipiranga 2752, 90610000, Porto Alegre, Brazil
silvia.guterres@ufrgs.br

Pharmazie 70: 155–164 (2015) *doi: 10.1691/ph.2015.4116*

The aim of this work was to develop solid lipid nanoparticles (SLN) containing copaiba oil with and without allantoin (NCOA, NCO, respectively) and to evaluate their antifungal activity. Nanoparticle suspensions were prepared using a high homogenisation technique and characterised by dynamic light scattering, laser diffraction, nanoparticle tracking analysis, multiple light scattering analysis, high-pressure liquid chromatography, pH and rheology. The antifungal activities of the formulations were tested *in vitro* against the emergent yeasts *Candida krusei* and *Candida parapsilosis*, and the fungal pathogens of human skin *Trichophyton rubrum* and *Microsporum canis*. The dynamic light scattering analysis showed z-average diameters (intensity) between 118.63 ± 8.89 nm for the nanoparticles with both copaiba oil and allantoin and 126.06 ± 9.84 nm for the nanoparticles with just copaiba oil. The D[4,3] determined by laser diffraction showed similar results of 123 ± 1.73 nm for the nanoparticles with copaiba oil and allantoin and 130 ± 3.6 nm for the nanoparticles with copaiba oil alone. Nanoparticle tracking analysis demonstrated that both suspensions had monomodal profiles and consequently, the nanoparticle populations were homogeneous. This analysis also corroborated the results of dynamic light scattering and laser diffraction, exhibiting a smaller mean diameter for the nanoparticles with copaiba oil and allantoin (143 nm) than for the nanoparticles with copaiba oil (204 nm). The physicochemical properties indicated that the dispersions were stable over time. Rheology evidenced Newtonian behaviour for both suspensions. Antifungal susceptibility showed a MIC_{90} of 125 μg/mL (nanoparticles with copaiba oil) and 7.8 μg/mL (nanoparticles with copaiba oil and allantoin) against *C. parapsilosis*. The nanoparticles with copaiba oil and the nanoparticles with copaiba oil and allantoin presented a MIC_{90} of 500 μg/mL and 250 μg/mL, respectively, against *C. krusei*. The MIC_{90} values were 500 μg/mL (nanoparticles with copaiba oil) and 1.95 μg/mL (nanoparticles with copaiba oil and allantoin) against *T. rubrum*. Against *M. canis*, the nanoparticles with copaiba oil and allantoin had a MIC_{90} of 1.95 μg/mL. In conclusion, nanoencapsulation improved the antifungal activity of copaiba oil, which was enhanced by the presence of allantoin. The MICs obtained are comparable to those of commercial products and can represent promising therapeutics for cutaneous infections caused by yeasts and dermatophytes.

1. Introduction

The incidence of infections caused by opportunistic pathogens in immunocompromised patients has become an important public health issue because these dermatophytes cause invasive infections (Peres et al. 2010). Yeast species belong to the normal flora of the human body, but in some circumstances that include HIV positive patients, chemotherapy, organ transplantation, surgery for cosmetic reasons or catheter use, yeasts become opportunistic pathogens (Pfaller et al. 2004). Lately, medicine has faced more and more problems due to yeast and fungus resistance to the current therapeutic arsenal (Kontoyiannis et al. 2002). Indeed, the number of yeasts resistant to intrinsic azole derivatives substantially increased in recent years. For instance, various *Candida* species are genetically resistant to fluconazole (Ying et al. 2012), and some dermatophytes, such as *Trichophyton* and *Microsporum,* which are the most common etiological agents that cause dermatomycoses in keratinised skin tissue, have demonstrated an increase resistance to the available drugs in recent decades (Pfaller et al. 2004). Furthermore, treatment of dermatophytosis is usually long and costly (Peres et al. 2010). For these reasons, it is important to develop new formulations for the effective treatment of fungal infections. Considering the problems with the drugs currently available, the use of natural substances with antifungal action may be a viable alternative worth exploring (Singh et al. 2001, Sagrera et al. 2011,

Zhao et al. 2010). The copaiba oil from *Copaifera martii* was chosen in this work thanks to its various pharmaceutical properties. It was identified as an orally active antileishmanial drug (Dos Santos et al. 2011). Additionally, Brazilian copaiba oils showed bactericidal activity against gram-positive bacteria and moderate activity against dermatophytes (Dos Santos et al. 2008). *Copaifera multijuga* Hayne oil-resin was associated with ZnO,$Ca(OH)_2$ and applied on a dental cement and showed antibacterial activity thanks to this association (Vasconselos et al. 2008). Moreover, this *Copaifera multijuga* Hayne oil-resin is already used as antioxidant (Maciel et al. 2007), analgesic (Carvalho et al. 2005), anti-septic (Pieri et al. 2010), anti-inflammatory (Basile et al. 1993), wound healing agent (Paiva et al. 2002), antitumoral agent against melanoma cells (Lima et al. 2003) and antimutagenic (Maistro et al. 2005). Furthermore, copaiba oil has been demonstrated to inhibit the growth of *Escherichia coli, Staphylococcus aureus* and *Pseudomonas aeruginosa* (Mendonça et al. 2008). While several pharmaceutical properties of this oil have been observed, the antifungal activity has not been well-explored. Da Silva and co-workers proved in 2009 that the use of copaiba oil resin prevented the germination and the growth of a specific fungus, *Colletotrichum gloeosporioides*, but no other reports were found about the antifungal activities of copaiba oil against fungi or yeast.

Thus, for all the above-cited reasons, copaiba oil seems to be a promising candidate to treat dermatophytosis. The use of copaiba oil as an alternative therapy requires the development of a suitable pharmaceutical formulation to carry it. Nanoparticles are ideal for this purpose because, thanks to their effective delivery of several substances with therapeutic or cosmetic properties, they have become incontrovertible to the scientific and technological interests in the health sciences. These particles could improve the bioavailability of drugs by targeting molecules to specific sites and controlling their release (Schaffazick et al. 2003). Additionally, the nanoparticles can penetrate deeply into bacterial strains and yeasts, which allows for more effective elimination of the pathogens (Prucek et al. 2011).

Among different nanostructures, solid lipid nanoparticles (SLN) are innovative and promise to act against yeasts and dermatophytes thanks to deep cellular penetration, higher concentrations and longer retention times (Liu et al. 2012). Above all, their nanometric size would provide an advantage in terms of specificity and effectiveness to fungicidal or fungistatic drugs. These antifungal properties are still limited due to the current lack of knowledge in various areas of fungal pathogen biology. To address these problems, topical formulations containing copaiba oil were developed in the present work.

Taking into consideration the need to develop innovative formulations and to improve the cosmetic properties for a topical use, different substances are frequently associated with the active substance of interest. Allantoin, a chemical compound with the formula $C_4H_6N_4O_3$, is often used in this manner. Allantoin results from the degradation of uric acid and is a form of nitrogen excretion in mammals (except humans and certain other primates). This molecule is also found in plants such as comfrey (Mazzafera et al. 2008). Allantoin is used in cosmetology for its various properties, including keratolytic (Veraldi et al. 2008), moisturising and soothing (Muangman et al. 2011) and wound healing effects (Araújo et al. 2010) as well as protection against irritants. Despite the beneficial effects of allantoin on dermatological formulations, this compound has not yet been evaluated in anti-fungal compositions.

The objective of this study was the development of innovative solid lipid nanoparticles for copaiba oil delivery. Additionally, we aimed to analyse the influence of allantoin on the SLN formulations and to evaluate the antifungal effect of these formulations against yeasts and dermatophytes.

2. Investigations and results

2.1. Nanoparticle production and characterisation

Liquid suspensions containing nanoparticles made of copaiba oil were successfully produced using a hot high-pressure homogenisation technique. All the suspensions had a homogeneous and milky macroscopic appearance with a bluish aspect indicating that the nanoparticles in suspension were under Brownian motion (Kaur et al. 2008). Several methods for obtaining nanoparticles are described in the literature, but one of the most relevant is high-pressure homogenisation. Due to its facility, possible large-scale production, pressure, cycles and temperature, this method was used in this work according to the drug of interest. Another advantage of this method is the use of solid lipids, which can be melted to obtain emulsions (Müller et al. 2000). There is considerable scientific interest in the physicochemical characterisation of nanoparticles produced by this technology thanks to the independent variables of this method, which include homogenisation pressure, number of homogenisation cycles, surfactants chain length and drug loading (Zidan *et al*. 2011). Consequently, it is possible to design and achieve different nanoparticles sizes that can be produced by optimising homogenisation conditions (pressure and number of passes), emulsifier type and viscosities of the dispersal and aqueous phases (Qian et al. 2011).

For the NCOA and NCO suspensions, the averages of the pH were 5.53 ± 0.01 and 6.24 ± 0.11, respectively, and the values were significantly different ($P < 0.05$). Both of these two suspensions were acidic but the pHs were still appropriate for a stratum corneum application, which has no physiological change when submitted to a pH in the range of 3.5-8.5 (Thune et al. 1988, SZNITOWSKA et al. 2001). As a consequence, the produced solutions can be safely used for a topical application.

2.2. Dynamic light scattering and laser diffraction

The DLS intensity analysis of the formulations (Fig. 1) showed monomodal profiles with a low polydispersity of below 0.1 (Gaumet et al. 2008). This indicated the high homogeneity of nanoparticle populations for both the NCOA and NCO suspensions. Moreover, the z-average diameter values were very similar for both suspensions (Table 1).

The Dynamic Light Scattering (DLS) measures particle size by light diffusion of particles moving under Brownian motion and applies the Stoke-Einstein equation to express this in terms of size distribution (Kholodenko et al. 1995). These data are

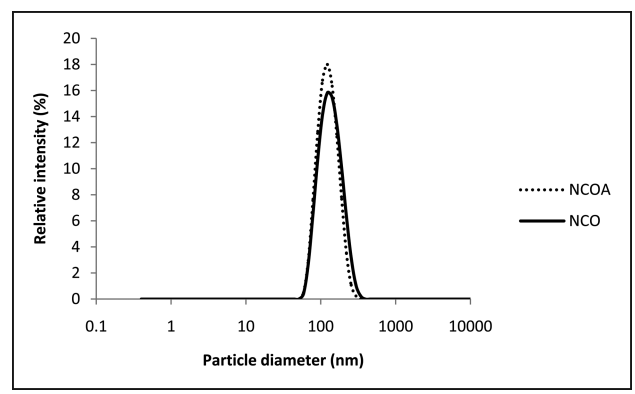

Fig. 1: Size distribution profiles by DLS considering light intensity of NCOA and NCO suspensions.

Table 1: Average diameter and polydispersion index of NCOA & NCO suspensions calculated by DLS

	Formulation	
	NCOA	NCO
z-average diameter (intensity) (nm)	118.6 ± 8.9	126.1 ± 9.8
PDI (intensity)	$0.07 \pm 0.01^*$	$0.11 \pm 0.04^*$

* values in the same row are significantly different ($P < 0.05$)

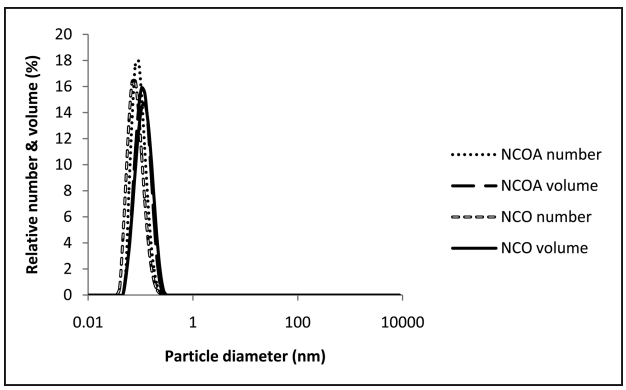

Fig. 2: Size distribution profiles by laser diffractometry considering number & volume of NCOA and NCO suspensions.

known as an intensity distribution, which is used to express the results because the particle scattering intensity is proportional to the sixth power of its diameter (Rayleigh's approximation). The Z-average size is the most significant and stable number calculated by the DLS technique. This technique is more accurate than laser diffraction for calculating nanometric diameters, but does not allow for detecting the presence of micrometric particles (Gaumet et al. 2008). Consequently, besides the DLS analysis, laser diffraction analysis was performed in addition to DLS analysis, confirming the absence of micrometric particles as observed in Fig. 2.

The diameters were expressed in terms of particle number and particle volume because each calculation allows for the assessment of different parameters. The mathematical relation between a particle diameter and its volume is cubic. For example, a 500 μm particle diameter is one million times more voluminous than a 5 μm particle diameter. If a suspension is composed by one particle of 500 μm and one million particles of 5 μm, the contribution of these two sizes to the entire distribution is identical for a volume size measure. If the value of the size measure is used, these one million particles of 5 μm contribute infinitely more to the overall distribution. Figure 2 shows that the results measured by number and volume are similar according to the observation on the graph, corroborating the values presented in Table 2.

Table 2: D[4,3] diameter and span polydispersion index of NCOA & NCO suspensions calculated by laser diffraction

	Formulation	
	NCOA	NCO
D[4,3] diameter (number) (nm)	$123.4 \pm 1.3^*$	$129.6 \pm 4.2^*$
Span (number)	$0.83 \pm 0.05^*$	$0.89 \pm 0.09^*$
D[4,3] diameter (volume) (nm)	$123.0 \pm 1.7^*$	$130.0 \pm 3.6^*$
Span (volume)	0.86 ± 0.05	0.93 ± 0.09

* values in the same row are significantly different ($P < 0.05$)

The Span expresses the range of the relative distribution to the median diameter, i.e., the homogeneity of the population. More homogenous suspensions have smaller Span values. The Span values were very similar for the NCOA and NCO suspensions whether they were determined by number or volume analysis, indicating a small distribution and homogenous populations of nanoparticles. These laser diffraction results corroborated the DLS results.

The results of particle size and distribution measured by Dynamic Light Scattering and laser diffraction were in accordance with other results, which demonstrated that it was possible to produce nanoparticles by high-pressure homogenisation with a low polydispersity. Moreover, the particle size distribution decreased when the number of passes and pressure increased (Qian et al. 2011). For Z-averages, there was no significant difference ($P < 0.05$) between NCOA (118.63 nm) and NCO (126.06 nm). The PDI values for NCOA (0.075) and NCO (0.106) were significantly different ($P < 0.05$). Concerning the D [4,3] by number and volume analysis, the differences were significantly different ($P < 0.05$) between NCOA and NCO. Additionally, Span values measured by number for the NCOA (0.831) and NCO (0.892) formulations were significantly different ($P < 0.05$). The volume calculations for NCOA (0.86) and NCO (0.934) were not significantly different ($P < 0.05$), as shown in Table 2. The average diameters were not significantly different ($P < 0.05$) when the DLS and the laser diffraction measurements for each suspension were used.

2.3. Nanoparticle tracking analysis

The Nanoparticle Tracking Analysis (NTA) technology was employed because it allows visualising, measuring and defining nanoparticles with high-resolution (Figs. 3 and 4).

The left curves represent the particle size in relation to the concentration, showing a mean diameter of 143 nm (NCOA, Fig. 3a) and 204 nm (NCO, Fig. 4a). It can be noted that the narrowness of the monomodal curves indicates the presence of homogeneous nanometric populations.

The middle graphs represent the particle size compared to the relative intensity of light. Two nanometric subpopulations can be observed in the NCOA suspension (Fig. 3b). The first has a diameter between 50 and 180 nm and the second between 180 and 280 nm. As for the NCO suspension, the Fig. 4b shows three nanometric subpopulations. The first has a diameter between 30 and 130 nm, the second is between 130 and 230 nm and the third is between 230 and 300 nm.

The right curves (Figs. 3c and 4c) show the particle size in relation to the relative intensity and the concentration. The populations were demonstrated to be homogeneous due to the narrow peaks. Moreover, the NCO population is less homogeneous than the NCOA population because the peak is wider, which corroborates the results obtained by DLS. The concentration measures gave values of 1.15×10^{14} particles/ml for the NCOA suspensions and 1.53×10^{12} particles/ml for the NCO suspensions.

The results verified by the NTA showed that the nanoparticles diameter varies from 50 to 280 nm for the NCOA suspension. The majority of these nanoparticles present a small light intensity. The subpopulation of nanoparticles that exhibits a greater light intensity are those with larger diameters, leading us to conclude that there is a small amount of crystal in this suspension. For the NCO population, the diameter fluctuates from 30 to 300 nm. Each of the three subpopulations shows an intensity proportional to its mean diameter. The highest value of relative light intensity of the NCOA suspension is twice as important as that of NCO. As with the NCOA liquid suspension, we can say that the NCO liquid suspension has a very small amount of crystals present.

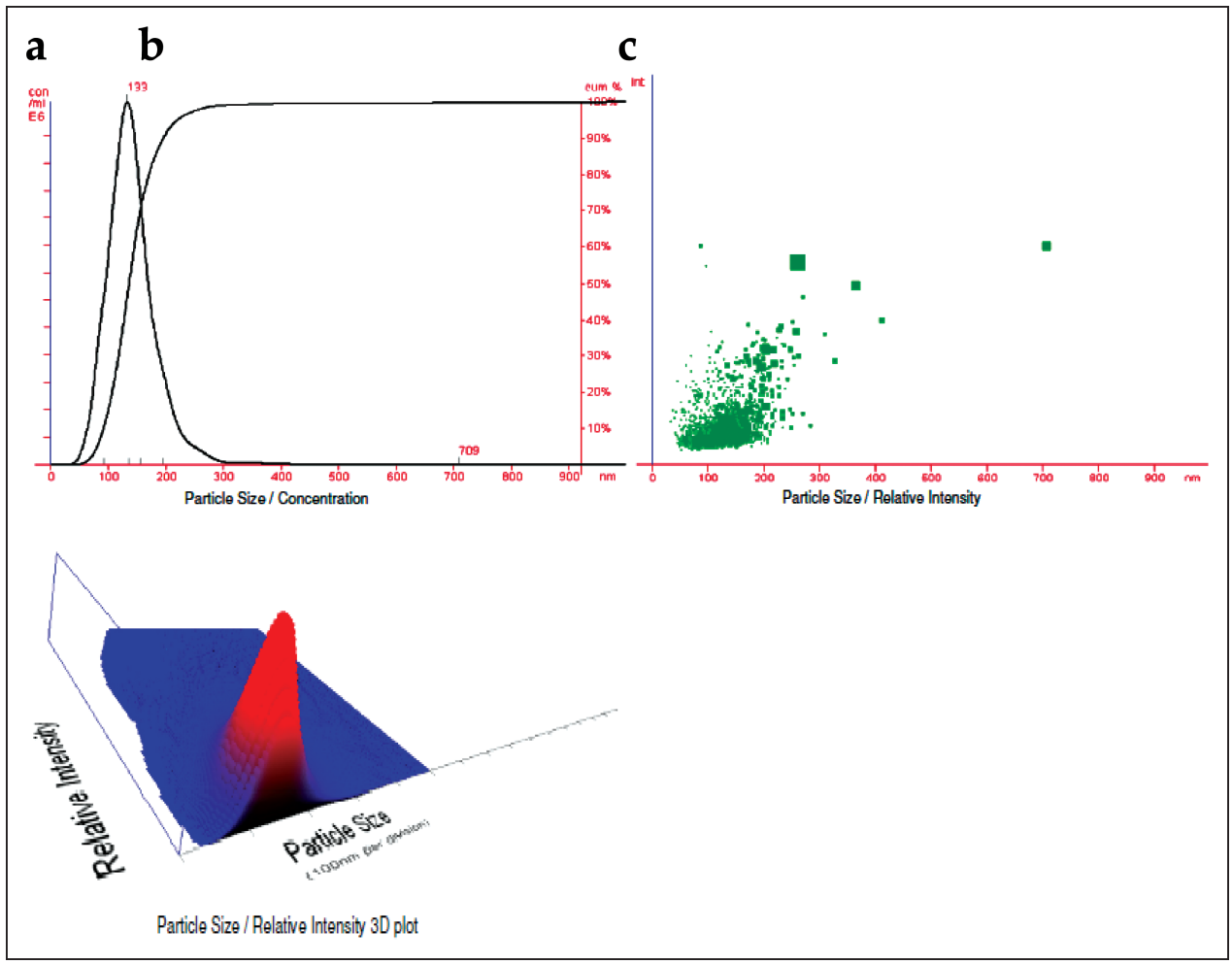

Fig. 3: NTA profile of NCOA suspension. a. Concentration = f(particle size). b. Relative light intensity = f(particle size). c. Concentration = f(particle size and relative light intensity).

2.4. Multiple light scattering

Multiple Light Scattering (MLS) is an optical method used to delineate concentrated liquid dispersions without dilution. MLS is performed by sending photons (NIR light source, 880 nm) into the sample. These photons, after being scattered various times by the particles in the dispersion, come out from the sample and are detected by the Turbiscan^{TM} reading head detectors. Backscattering is directly associated with the mean free path of photon transport and thus depends on particle size and concentration. This measurement principle is applied to detect particle size change and/or local concentration change during destabilisation of the sample (Turbiscan^{TM} technology and Static Multiple Light Scattering), (Celia et al. 2009; Külkamp-Guerreiro et al. 2012).

Time-dependent physical stability is one of the most important desired characteristics of a product (Araujo et al. 2011). Lipid nanoparticles are heterogeneous, thermodynamically unstable systems and therefore they have a significant tendency to lose physical stability during storage (Huang et al. 2008). The literature reports, however, that lipid nanoparticle dispersions with optimised stabiliser compositions are physically stable in storage for several years (Bunjes et al. 2003). The Turbiscan^{TM} instrument allows distinguishing between the two major destabilisation phenomena affecting the homogeneity of dispersions: particle migration (creaming, sedimentation), which is reversible by mechanical stirring, and particle size variation or aggregation (coalescence, flocculation), which is often irreversible (Mengal et al. 1999).

Figure 5 and Fig. 6 show the delta backscattering of NCOA and NCO suspensions, respectively. Variations of the delta backscattering intensity over time are visible at the extremes of the profiles while no variation is observed in the middle of the same profiles. These results allowed us to conclude that the size variations were insignificant due to the delta backscattering intensities of NCOA and NCO, which varied in a range smaller than the -5% to + 5% range required for a stable suspension (Celia et al. 2009; Külkamp-Guerreiro et al. 2012). Consequently, both suspensions (NCOA and NCO) were considered physically stable due to the small range of variation in the delta backscattering intensity.

On the other hand, these time-dependent variations indicated migration phenomena, which meant that various nanoparticles movements were most likely the consequence of different nanoparticles diameters. Furthermore, the different movements owing to the different diameters were reversible.

2.5. Allantoin content

The presence of allantoin in the aqueous phase of the formulations was measured by HPLC. Copaiba oil, present in the internal phase, has not been quantified because it is a complex mixture of many components (Veiga Junior et al. 2007). The linear relationship of peak area versus concentration of standard suspension was calculated to obtain equation 3, where Y is the peak area and X is the allantoin concentration (μg/ml):

$$Y = 25031X + 5542 \quad (3)$$

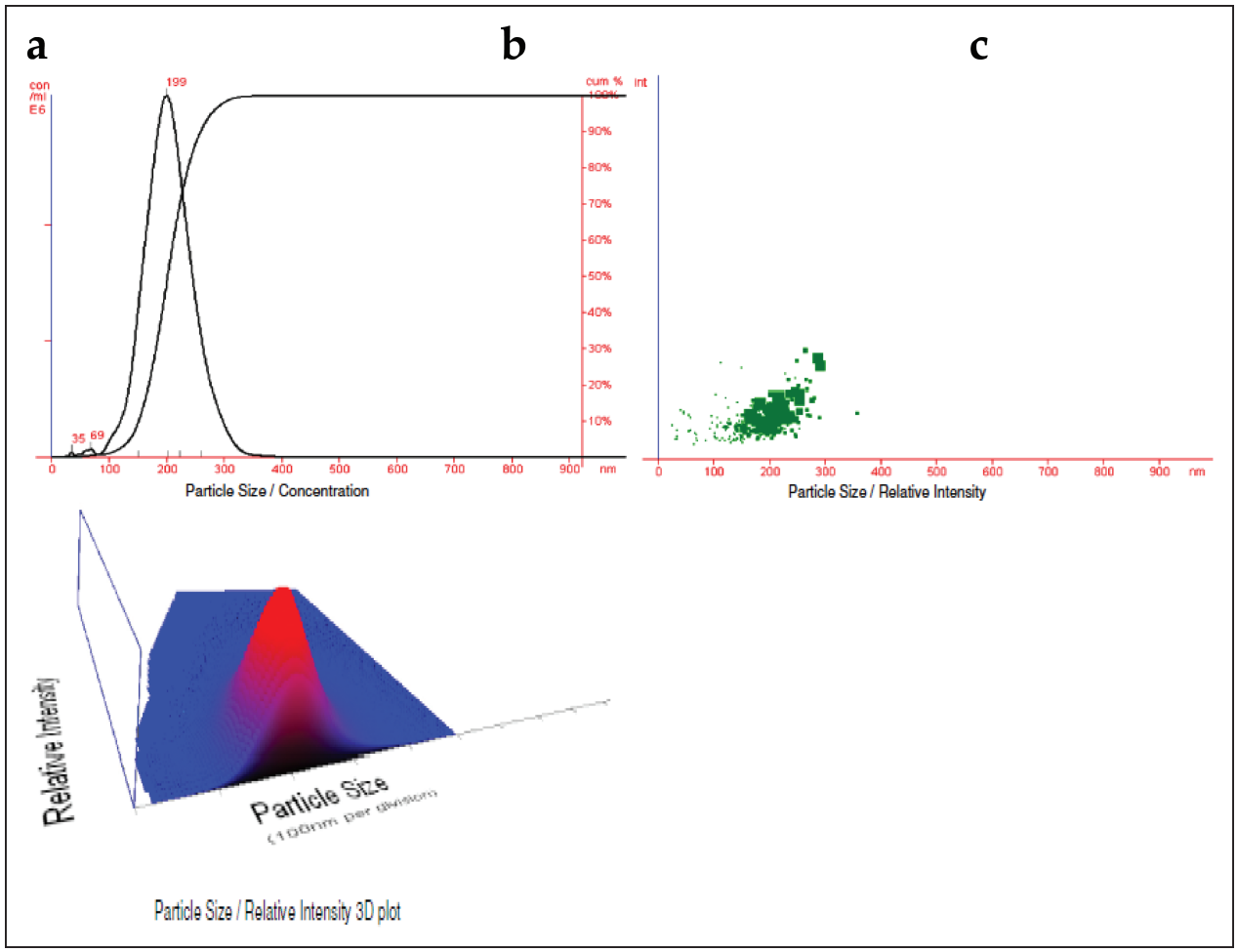

Fig. 4: NTA profile of NCO suspension. a. Concentration = f(particle size) b. Relative light intensity = f(particle size) c. Concentration = f(particle size and relative light intensity).

The determined linearity was verified by regression analysis using a seven-point measurement and correlation coefficient of $r^2 > 0.9982$. The precision of this method was determined and the results showed a repeatability of 1.44% and an intermediate precision of 1.65%. The accuracy results exhibited a recovery average of $95.02 \pm 3.37\%$, demonstrating the specificity of the method. The results allow us to conclude that it was possible to detect allantoin. Moreover, the method used in this study was demonstrated to be effective and appropriate for quantifying allantoin (Haghi et al. 2008). The results obtained from NCOA formulations demonstrated that 80.4% of the total allantoin was free and that only 19.6% of the allantoin content was in the external aqueous phase.

2.6. *Rheology study*

Both the NCOA and NCO suspensions showed a linear relation between the different shear rates and the different shear stresses. Thus, it was possible to conclude the two suspensions were Newtonian fluids because according to the Newton law, a fluid is considered to be Newtonian if the shear stresses are directly proportional to the shear rates. Consequently, the

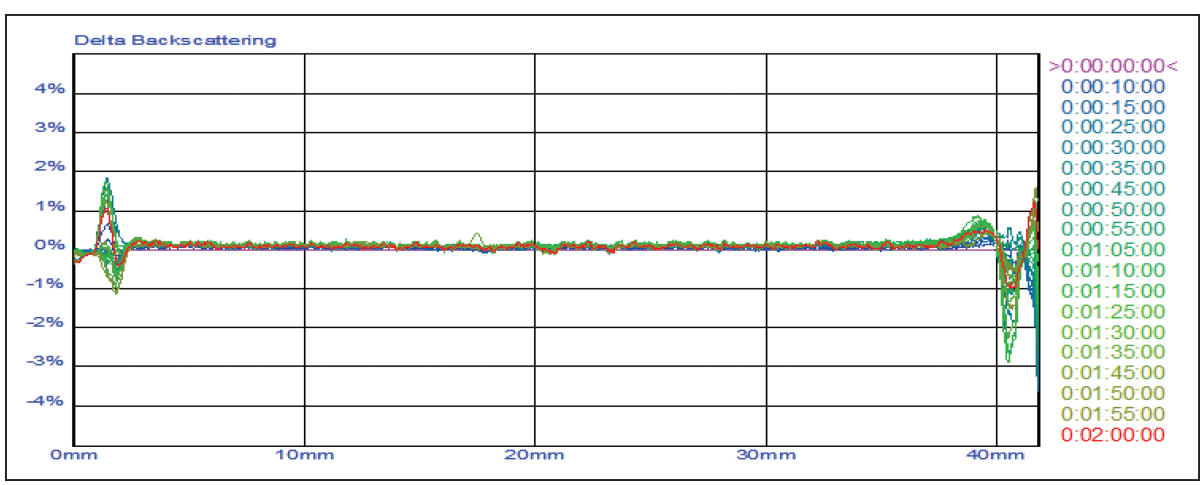

Fig. 5: Delta backscattering intensity profile of NCOA suspension.

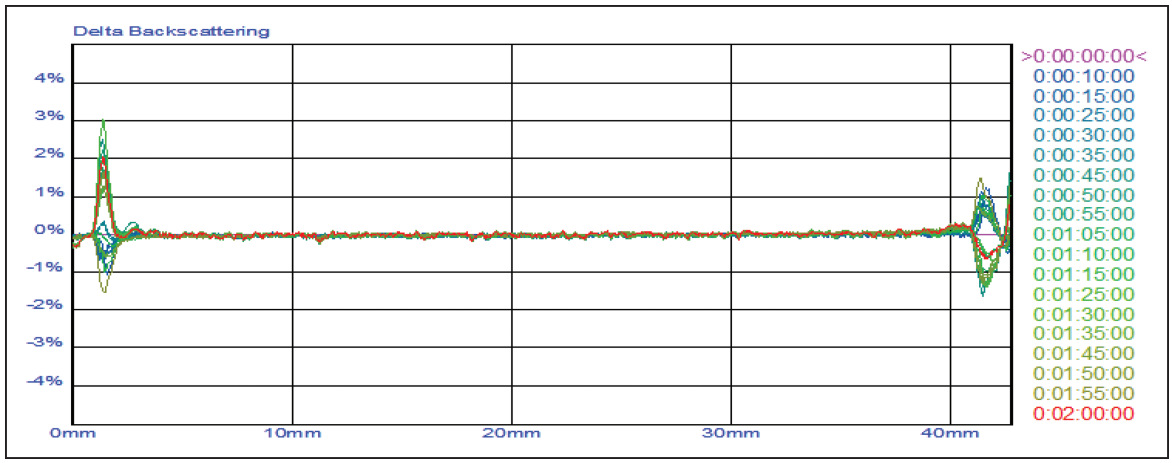

Fig. 6: Delta backscattering intensity profile of NCO suspension.

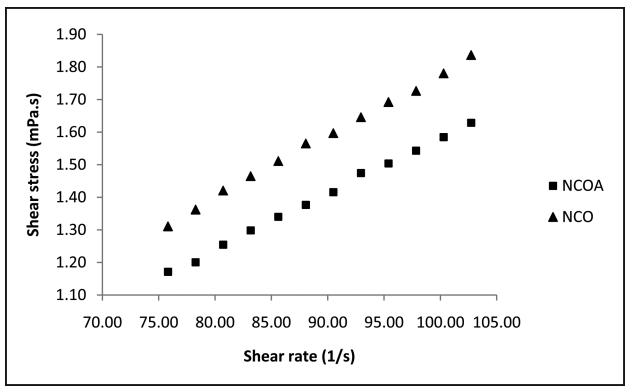

Fig. 7: Rheogram of NCOA and NCO suspensions.

viscosity is independent of the applied shear. On the contrary, non-Newtonian fluids have shear stresses which are not proportional to the shear rates and furthermore have much more complex physical behaviours.

The values of the flow index (η) were close to 1 for the two suspensions. These results corroborated the Newtonian behaviour of NCOA and NCO because according to the Power Law Model, the flow index must be close to the value of 1 (Mccarthy et al. 2011). Thus, we concluded that the addition of allantoin did not modify either the viscosity or the flow rate. Both suspensions are good candidates for topical use due to their stability and the characteristics of their rheological properties.

2.7. Antifungal activity evaluation of pure copaiba oil and copaiba oil/allantoin-loaded nanoparticles by broth microdilution assay

The results of the antifungal tests demonstrated that none of the microorganisms were susceptible to solutions of free copaiba oil (SCO) or to free allantoin (SA) (Table 4).

Candida krusei CKR 01 and *Candida parapsilosis CPA 05* were susceptible to NCO, which had a fungistatic activity. The NCOA suspensions showed a higher fungistatic activity for *Candida krusei CKR 01* and *Candida parapsilosis CPA 05* and showed a fungicidal activity for *Candida parapsilosis CPA 05*.

The *Trichophyton rubrum TRU 31* was susceptible to NCO, which demonstrated a fungistatic activity. The susceptibility was even higher to NCOA, which showed both fungistatic and

Table 3: Mean values and standard deviations of flow index (η), obtained through application of Power Law model, and viscosity values in a fixed velocity of 72 rpm

Suspensions	Number of suspensions	Repetitions	Flow index (η)	Viscosity (mPa.s)
NCOA	2	3	1.020 ± 0.023	$1.57 \pm 0.016^{*}$
NCO	2	3	1.046 ± 0.011	$1.76 \pm 0.016^{*}$

*values in the same row are significantly different ($P < 0.05$)

Table 4: *In vitro* susceptibility of free copaiba oil (SCO), free allantoin (SA), NCOA and NCO against yeasts and dermatophytes species of clinical interest.

Fungal species	SCO	SA	NCOA		NCO	
			FG	FS	FG	FS
Candida krusei CKR 01	–	–	–	250	–	500
Candida parapsilosis CPA 05	–	–	62.5	7.8	–	125
Trichophyton rubrum TRU 31	–	–	3.9	1.95	–	500
Microsporum canis MCW3	–	–	3.9	1.95	–	–

The results were expressed as MIC_{90} (μg/ml): MIC values which inhibit 90% of the isolates.
(–): no antifungal activity. FG: fungicide activity. FS: fungistatic activity.

fungicidal activities. *Microsporum canis MCW3* was susceptible only to NCOA, which showed both fungistatic and fungicidal activities.

This study demonstrated that both suspensions had an antifungal activity on the yeasts and dermatophytes tested. The results showed that the NCOA suspension was more effective than the NCO suspension. The NCOA suspension presented fungicidal and fungistatic activities at much lower concentrations than the NCO suspension. The mycological results of this work proved the MIC_{90} values for the NCOA suspensions were higher than those obtained with itraconazole, which presented antifungal activity against *C. krusei* and *C. parapsilosis* with $MICs_{90}$ of 0.250 μg/ml and 0.036 μg/ml, respectively. In the same study, voriconazole presented an activity against *C. krusei* and *C. parapsilosis* with a MIC_{90} of 0.060 μg/ml and 0.030 μg/ml, respectively (Marcos-Arias et al. 2011). In the same way, the essential oil from the seed of *Anethum graveolens* has a demonstrated fungicidal activity against *C. krusei* and *C. parapsilosis* with a MIC of 0.312 μg/ml (Hong et al. 2011). Once more, these results denoted lower MICs than in the present study.

Park et al. (2011) demonstrated the antifungal activity of epigallocatechin 3-O-gallate against *T. rubrum* and *M. canis* with MIC_{90} values of 8.0 μg/ml and 4.0 μg/ml, respectively. In this work, the value of 3.9 μg/ml was smaller and equal for both species. Infections of hair, skin and nails have increased considerably among paediatric and geriatric populations (Mukherjee et al. 2003); (Monod et al. 2008). Such infections are primarily caused by *T. rubrum* and other dermatophytes and are not life-threatening; however, both immunocompetent and immunosuppressed persons are affected (Vermount et al. 2008). Chronic skin infections carry considerable morbidity and can become serious in immunocompromised patients, resulting in invasive infections (Sokovic et al. 2006). Thus, *T. rubrum* is very important in terms of public health. The MIC_{90} result found in this study, 3.9 μg/ml, is similar to those showed by Aala et al. (2010) for the inhibition of *T. rubrum* by allicin (8.12 μg/ml), ketoconazole (2.75 μg/ml) and fluconazole (11.4 μg/ml). Mota et al. (2009) obtained MIC_{90} values for fluconazole of 32 μg/ml against *T. rubrum* and 16 μg/ml against *M. canis*. For ketoconazole, MIC_{90} values of 4 μg/ml (*T. rubrum*) and 0.25 μg/ml (*M. canis)* were obtained, and terbinafine presented MIC_{90} values equal to 0.25 μg/ml for both dermatophytes. In this work, the values obtained were 3.9 μg/ml for both NCOA and NCO. In conclusion, NCO was less efficient than ketoconazole and terbinafine but more efficient than fluconazole. Dos Santos and co-workers (2008) showed that the antifungal activity of copaiba oil depends on the species of the Copaifera genus. In this work, oils from *C. paupera* and *C. lucens* were demonstrated to exhibit light activity against *T. rubrum* and *M. canis*, and those from *C. cearensis*¸ *C. langsdorffii* and *C. multijuga* showed moderate activity against only *T. rubrum* (MIC = 250-500 μg/ml).

3. Discussion

Stable formulations of solid lipid nanoparticles containing copaiba oil with and without allantoin were produced. Our results showed that it was possible to obtain nanoparticles with a low polydispersity and narrow, monomodal profiles, indicating high homogeneity. The chosen parameters for the hot high-pressure homogenisation (3 cycles and 400 bars pressure) allowed for the creation of homogenous nanoparticles.

The antifungal activity opens new perspectives against infections caused by yeasts and dermatophytes thanks to the MICs values, which were similar to, or even lower than, some commercial antifungal products. The findings of this study are important due to the strong multidrug-resistance of the fungi tested in this work. Finally, the nanoencapsulation technology associated with the copaiba oil demonstrated its effectiveness in terms of drug delivery and antifungal activity against some clinical and resistant yeasts and dermatophytes.

4. Experimental

4.1. Chemicals and solvents

Copaiba oil was supplied by Inovam (Brazil), cetyl palmitate by Cognis (Germany), allantoin and butyl hydroxy toluene (BHT) by Viafarma (Brazil), Span 80 and Tween 80 were supplied by Oxiteno (Brazil). All these products presented pharmaceutical grade. All other solvents and chemicals were of analytical grade and all reagents were used as received.

4.2. Preparation of solid lipid nanoparticles

Formulations of solid lipid nanoparticles containing copaiba oil (NCO) were prepared using hot high pressure homogenisation as described by Müller et al. (2000). Formulations with allantoin (NCOA) were also produced. For the lipid phase, copaiba oil (6 g) was mixed with cetyl palmitate (12 g). Then, Span 80 (2 g) and BHT (0.1 g) were added to the mixture. For the aqueous phase, Tween 80 (4 g) was added to milli-Q water (175.9 g). For the NCOA dispersions, allantoin (2 g) was added and diluted in the aqueous phase. Both the lipid and aqueous phases were heated at 80-85 °C for 30 min. Afterwards, the aqueous and lipid phases were mixed under high stirring (11,000 rpm for 1 min, then 13,000 rpm for 1 min and finally 16,000 rpm for 3 min) using an Ultra-Turrax (T25, Ika). The obtained pre-emulsion was homogenised under high pressure (Panda 2KNS 1001 L, Saovi Niro). For homogenisation, 3 cycles of 400 bars were applied for all the formulations. Then, the oil/water nanoemulsions produced were cooled to 25 °C, thereby allowing the recrystallisation of the lipids and resulting in the NCO or NCOA formulations in compliance with the initial compositions. Both of the suspensions were produced in triplicate.

4.3. Characterisation of the nanoparticle formulations

4.3.1. Dynamic light scattering and laser diffraction

Particle size was determined by calculating the average diameter (z-average) and polydispersity index (PI) by Dynamic Light Scattering (DLS) with a Zetasizer Nano ZS (Malvern Instruments, UK). Each test was performed in triplicate at 25 °C after a 1/5000 (v/v) dilution with ultra-purified water. The results were expressed in terms of particles intensity.

Laser diffraction (LD) (Mastersizer® model 2000, Malvern Instruments, UK) was used to discard the presence of particles above 1 μm. Three measurements were carried out for the suspensions and the averages were calculated. The diameter results were expressed in terms of D [4,3], which considers particles volume and represents the average diameter expressed by the volume of the corresponding sphere. This technique was also used to determine the distribution width based on the 10%, 50% and 90% quantile. These were represented by the Span values according to Eq. (1), in which D[v, 0.9], D[v, 0.1], D[v, 0.5] are the diameters at which 90%, 10% or 50% of the distribution was below, respectively.

$$\text{Span value} = D[v, 0.9] - D[v, 0.1]/D[v, 0.5] \quad (1)$$

4.3.2. Nanoparticle tracking analysis

The formulations were also analysed by Nanoparticle Tracking Analysis (NTA) technology (NanoSight©) in order to determine high-resolution particle size distributions. NTA also furnishes real time monitoring of the nanoparticle populations, detects and visualises populations of nanoparticles in liquids down to 10 nm depending on the material, and measures the size of each particle from direct observations of diffusion. A microscope based system linked to a CCD camera, which recorded and validated all data with video files at 30 frames per second, was used to observe particles moving under Brownian motion within the path of the laser beam. Finally, the concentration, particle diameter and diffusion coefficient were calculated. (Moddaresi et al. 2010). Analyses were carried out after the mass fraction of the formulation was calculated. Finally, a 1/5000 (v/v) dilution was performed for each dispersion.

4.3.3. Multiple light scattering

Multiple Light Scattering (MLS) technology was used to detect particle size aggregation and local concentration of particles within the sample in order to assess the physicochemical stability (Formulation Company for Turbiscan™ technology and Static Multiple Light Scattering). The principal

advantage of Turbiscan^{TM} is the capacity to detect destabilisation phenomena earlier than the human eye, especially for opaque systems. Samples of 10 ml from each suspension were poured carefully into a cylindrical glass cell to obtain a clear and proper meniscus. Measurements were made every 5 min for 2 h.

4.3.4. Quantification of allantoin by HPLC and pH determination

The allantoin content in NCOA formulations was determined by high performance liquid chromatography (HPLC), using a Perkin Elmer Series 200 HPLC equipped with a Series 200 autosampler, a UV/VIS detector and a Phenomenex Luna 5 μ C18(2) column (150 mm × 4.60 mm, 5 μm). The mobile phase consisted of 0.03 mol·L^{-1} NaH_2P0_4 in water/methanol (90:10, v/v) solution at a flow rate of 0.4 mL·min^{-1}. Direct UV detection was performed by absorbance at 224 nm. The validation of the method was assessed by linear regression of three identical curves within the range of 5 to 35 μg/mL. The precision of the method was determined by testing six independent samples of a fresh preparation at 100% of the test concentration (20 μg/mL) repeated on different days. The values of the intra-day relative standard deviation% [R.S.D.(%)] were obtained from the first day results and were used to measure method repeatability. The average inter-day R.S.D.(%) values collected from the results of both days were used to evaluate intermediate precision. Accuracy was determined by recovering tests that were performed on all samples. The recovery consisted of adding known amounts of allantoin to the sample. The per cent recovery (%R) was calculated. The specificity was assessed by injecting allantoin-free formulations prepared using the same procedure.

The validated method was used to determine the total allantoin content in the NCOA formulation, which was diluted in a 0.03 mol·L^{-1} NaH_2P0_4 in water/methanol (90:10, v/v) solution to reach a theoretical allantoin concentration of 20 μg/mL. The solution was then stirred with a magnetic bar for 5 min, filtered using a 0.45 μm filter (Millipore) and injected at a volume of 40 μL.

To determine the quantity of non-nanoencapsulated allantoin, the ultrafiltration-centrifugation technique was employed using membranes (Amicon Ultra 10,000 Da) from Millipore (USA). A volume of 500 mL of NCOA was centrifuged at 2,150 *g* for 5 minutes at a temperature of 25 °C. Then, the peak area of the ultrafiltered portion was measured to determine the free allantoin concentration.

Finally, the pH of each dispersion was measure using a calibrated Digimed DM-22 pH meter. Each measurement was carried out in triplicate.

4.4. Rheology study

The viscosities of both suspensions were measured with a Brookfield rotational viscometer DV-II + Pro in LVF mode and with a CS4-25 spindle. The rheological parameters were obtained in triplicate with samples kept at 25 ± 1 °C. To define the fluid behaviours as either Newtonian or non-Newtonian, the relationship between shear rates and shear stresses were analysed. The results were expressed with rheograms and analysed by the Power Law Model, which was applied thanks to its facility and efficacy in describing the rheological phenomena (Bird et al. 1960). In this mathematical model, shear stresses are plotted versus shear rates, and the slope of the obtained straight line allows for the calculation of the flow index (Lieberman et al. 1996). This permits one to determine the Newtonian or non-Newtonian behaviour of the fluids. The Power Law model is represented by Eq. (2) in which the shear stress (τ) is given by the flow consistency index (k), the shear rate (γ) and the flow behaviour index (η).

$$\tau = k\gamma^{\eta} \quad (2)$$

4.5. Fungal strains and activity evaluation of pure copaiba oil and nanoencapsulated by broth micro dilution assay

For this work, two species of yeast (*Candida krusei* CKR01 and *Candida parapsilosis* CP05)and two dermatophyte species (*Trichophyton rubrum* TRU31 and *Microsporum canis* MCW3)were tested. The fungal isolates exhibit multidrug-resistance to fluconazole, anidulafungin, ketoconazole and griseofulvin. All fungal strains are deposited in the Mycology Collection of the Universidade Federal do Rio Grande do Sul. The antifungal susceptibility testing was assessed according to the Clinical and Laboratory Standard Institute (CLSI) documents M38-A2 (2008) for dermatophytes and M27-S4 (2012) for yeasts. The yeast inoculums were prepared from a pure yeast culture for 24 h, equivalent to a visual turbidity of 0.5 on the MacFarland scale corresponding to 10^6 UFC/mL. The turbidity of the dermatophyte inoculums was determined by spectrophotometry, in which a transmittance of 80-82% was obtained, corresponding to a range of 0.4×10^4 at 5×10^4 cells/mL. All tests were performed in 96-well plates and expressed as the Minimal Inhibitory Concentration (MIC_{90}), which refers to both the concentration able to inhibit 90% of the isolates and the minimal fungicidal concentration (MFC).

To determine MIC_{90} values, fungal inoculums were diluted to a total volume of 500 μg/ml in each well with Roswell Park Memorial Institute medium-morpholino propane sulfonic acid (RPMI-MOPS), which consisted of RPMI 1640 containing L-glutamine without sodium bicarbonate (Sigma-Aldrich Co., St Louis, MO, USA) buffered to pH 7.0 with 0.165 mol·L^{-1} MOPS-Sigma buffer. The sterility of the medium was controlled by adding only culture medium to these wells. To check for a possible interference between the surfactant Tween 80 (Sigma), which was used to solubilise the compounds, a concentration equivalent to that present in the solution was added to this well and was verified by the presence of microorganisms. In addition, we used a commercial antifungal terbinafine (from Cristalia®) at a concentration of 32 μg/mL as a control inhibitor.

After the incubation period, the reading of the presence or absence of inhibition was visually performed and confirmed with polo-box binding domain (PBD) resazurin 0.01%, which acts as an intermediate electron acceptor in the electron transport chain between the final reduction of oxygen and cytochrome oxidase. The resazurin assay is used to assess bacterial or yeast contamination, has no toxicity to cells and does not need to kill cells in order to achieve measurement (Perrot et al. 2003). It is a simple and rapid colorimetric and metabolic test in which a 0.01 mg/mL solution is added to the medium. Resofurin is the deoxygenated product of resazurin that is colorimetrically measured because it exhibits a strong emission at wavelengths higher than 550 nm. Aliquots of 10 μL were plated on Sabouraud agar to define the fungicidal or fungistatic inhibition. The tests were performed in triplicate, and the microplates were incubated at 32 °C for 48 h. The concentration range of the copaiba oil varied from 500 μg.ml^{-1} to 1.95 μg.ml^{-1}.

The MFC was determined by subculturing 10 μl aliquots of all wells onto plates containing Sabouraud Dextrose Agar (Merck, Germany), which were incubated at 32 °C for 48 h. The lowest concentration of copaiba oil at which negative growth was recorded was considered to be the MFC.

All the isolates were tested in duplicate. NCOA and NCO suspensions were diluted in aqueous solution with Tween 80 (2%) to obtain a concentration of 1 mg/ml of copaiba oil. To verify the antifungal activity of pure copaiba oil (SCO) and pure allantoin (SA), two solutions were prepared with the same solvent to obtain a concentration of 1 mg/ml for both of these two substances.

All the isolates were tested in duplicate. NCOA and NCO suspensions were diluted in aqueous solution to obtain a concentration of 1 mg/ml of copaiba oil. To control for a possible interference by Tween 80, which was used as a surfactant for solubilising the compounds, a concentration equivalent to the ones present in the suspensions was added to this well. The presence of microorganisms was simultaneously checked. To verify the antifungal activity of pure copaiba oil (SCO) and pure allantoin (SA), two aqueous solutions were prepared. One solution contained only copaiba oil while the other contained allantoin at concentrations equivalent to those of the NCOA and NCO suspensions. The presence or absence of inhibition was determined visually. Aliquots (10 μL) were plated on Sabouraud agar and incubated for 2 days at 32 °C to define the fungicide or fungistatic inhibition. Growth confirmed fungistatic inhibition while the absence of growth confirmed fungicidal inhibition.

4.6. Statistical analysis

The values of average diameter, polydispersity index, pH, flow behaviour index and viscosity were analysed using a statistical T-test, which was performed with two samples assuming equal variances. These analyses were performed using the Microsoft Excel® 2010 Software (Microsoft® Corporation, USA).

The statistical significance of antifungal activity results was performed with the Independent-Samples Kruskal-Wallis test using the software IBM SPSS 18®. Differences were considered significant at p values of less than 0.05.

Acknowledgements: The authors wish to acknowledge the National Council for Scientific and Technological Development (CNPq, Brazil), CAPES (Coordenação de Aperfeiçoamento de Pessoal de Nível Superior) and o PRONEX/FAPERGS-CNPq e a Rede Nanotecnolgia Farmacêutica CAPES for financial support and Professor Patricia Ziegelmann (UFRGS) for assistance with the statistical analysis.

References

Aala F, Yusuf UK, Jamal F, Khodavandi A (2010) *In vitro* antifungal activity of allicin alone and in combination with two medications against *Trichophyton rubrum*. World J Microbiol Biotechnol 26: 2193–2198.

Araújo J, Nikolic S, Egea MA, Eliana B, Souto EB, Garcia ML (2011) Nanostructured lipid carriers for triamcinolone acetonide delivery to

the posterior segment of the eye. Colloids Surfaces: Biointerfaces 88: 150–157.

Araújo LU, Grabe-Guimarães A, Mosqueira VCF, Carneiro CM, Silva-Barcellos NM (2010) Profile of wound healing process induced by allantoin. Acta Cirúrgica Brasileira 25: 460–466.

Basile AC, Sertié JAA, Freitas PCD, Zanini AC (1988) Anti-inflammatory activity of oleoresin from Brazilian copaifera. J Ethnopharmacol 22: 101–109.

Bird RB, Stewart WE, Lightfoot EN (1960) Transport Phenomena. John Wiley, New York 920.

Bunjes H, Koch MH, Westesen K (2003) Influence of emulsifiers on the crystallization of solid lipid nanoparticles. J Pharm Sci 92: 1509–1520.

Carvalho JCT, Cascon V, Possebon LS, Morimoto MSS, Cardoso LGV, Kaplan MAC, Gilbert B (2005) Topical antiinflammatory and analgesic activities of *Copaifera duckei* dwyer. Phytother Res 19: 946–950.

Celia C, Trapassob E, Coscoa D, Paolinoc D, Fresta M (2009) Turbiscan Lab® Expert analysis of the stability of ethosomes® and ultradeformable liposomes containing a bilayer fluidizing agent. Colloids Surfaces B: Biointerfaces 72: 155–160.

Clinical laboratory standards institute (CLSI) (2008): Reference method for broth dilution antifungal susceptibility testing of filamentous fungi: approved standard – Second Edition. CLSI document M38-A2. Wayne: Clinical Laboratory Standards Institute.

Clinical laboratory standards institute (CLSI) (2012): Reference Method for Broth Dilution Antifungal Susceptibility Testing of Yeasts: Fourth Informational Supplement, CLSI document M27-S4. Clinical and Laboratory Standards Institute, Wayne, PA, USA.

Da Silva AC, Sales NDP, De Araujo AV, Caldeira CF (2009) *In vitro* effect of plant compounds on the fungus *Colletotrichum gloeosporioides* Penz. isolated from passion fruit. Ciencia Agrotecnol 33: 1853–1860.

Dos Santos AO, Ueda-Nakamura T, Filho BPD, Júnior VFV, Pinto AC, Nakamura CV (2008) Antimicrobial activity of Brazilian copaiba oils obtained from different species of the *Copaifera* genus. Memórias do Instituto Oswaldo Cruz, Rio de Janeiro 103: 277–281.

Dos Santos AO, Costa MA, Ueda-Nakamura T, Filho BPD, Júnior VFV, Lima MMS, Nakamura CV (2011) Leishmania amazonensis: Effects of oral treatment with copaiba oil in mice. Exper Parasitol 129: 145–151.

Fava LW, Serpa PBS, Külkamp-Guerreiro IC, Pinto AT (2013) Evaluation of viscosity and particle size distribution of fresh, chilled and frozen milk of Lacaune ewes. Small Ruminant Res 113: 247–250.

Gaumet M, Vargas A, Gurny R, Delie F (2008) Nanoparticles for drug delivery: The need for precision in reporting particle size parameters. Eur J Pharm Biopharm 69: 1–9.

Haghi G, Arshi R, Safaei A (2008) Improved high-performance liquid chromatography (HPLC) method for qualitative and quantitative analysis of allantoin in *Zea mays*. J Agricult Food Chem 56: 1205–1209.

Hong Z, Jun T, Yuechen Z, Xiaoquan B, Jingsi Z, Yehong M, Youwei W (2011) *In vitro* and *in vivo* activities of essential oil from the seed of *Anethum graveolens* L. against *Candida* spp. Evid-Based Complement Altern Med 2011: 659704.

Huang ZR, Hua SC, Yang YL, Fang JY (2008) Development and evaluation of lipid nanoparticles for camptothecin delivery: a comparison of solid lipid nanoparticles, nanostructured lipid carriers, and lipid emulsion. Acta Pharmacol Sin 29: 1094–1102.

Kaur IP, Bhandari R, Bhandari S, Kakkar V (2008) Potential of solid lipid nanoparticles in brain targeting. J Control Release 127: 97–109.

Kholodenko AL, Douglas JF (1995) Generalized Stokes-Einstein equation for spherical particle suspensions. Physical Review 51: 1081–1090.

Kontoyiannis DP, Lewis RE (2002) Antifungal drug resistance of pathogenic fungi. Lancet 359: 1135–1144.

Külkamp IC, Paese K, Guterres SS, Pohlmann AR (2009) Stabilization of lipoic acid by encapsulation in polymeric nanocapsules planned for dermal application. Quimica Nova 32: 2078–2084.

Külkamp-Guerreiro IC, Terroso TF, Assumpção ER, Berlitz SJ, Contri RV, Pohlmann AR, Guterres SS (2012) Development and stability of innovative semisolid formulations containing nanoencapsulated lipoic acid for topical use. J Nanosci Nanotechnol 12: 1–10.

Lieberman JA, Rieger MM, Banker GS (1996) In: Rheological and Mechanical Properties of Dispersed Systems in Pharmaceutical Dosage Forms. Disperse Systems 1, 2nd ed., Radebaugh, New York, p. 552.

Lima SR, Junior VF, Christo HB, Pinto AC, Fernandes PD (2003) *In vivo* and *in vitro* studies on the anticancer activity of *Copaifera multijuga* Hayne and its fractions. Phytother Res 17: 1048–1053.

Maciel HPF, Gouvêa CMCP, Toyama M, Smolka M, Marangoni S, Pastore GM (2007) Extraction, purification and biochemical characterization of a peroxidase from *Copaifera langsdorffii* leaves. Quimica Nova 30: 1067–1071.

Maistro EL, Carvalho JCT, Cascon V, Kaplan MAC (2005) *In vivo* evaluation of the mutagenic potential and phytochemical characterization of oleoresin from *Copaifera duckei* Dwyer. Genet Mol Biol 28: 833–838.

Marcos-Arias C, Eraso E, Madariaga L,Carrillo-Muñoz AJ, Quindós G (2012) *In vitro* activities of new triazole antifungal agents, posaconazole and voriconazole, against oral *Candida* isolates from patients suffering from denture stomatitis. Mycopathologia 173: 35–46.

Mazzafera P, Goncalves KV, Shimizu MM (2008) Control of allantoin accumulation in comfrey. Nat Prod Comm 3: 1411–1422.

McCarthy OJ (2011) Rheology of liquid and semi-solid milk products. In: Fuquay JW, Fox PF, Mcsweeney PLH. (ed) Encyclopedia of Dairy, Sciences 4, 2nd ed., Elsevier, London, p. 520–531.

Mota CRA, Miranda KC, Lemos JA, Costa CR, Hasimoto e Souza LK, Passos XS, Meneses e Silva H, Silva MRR (2009) Comparison of *in vitro* activity of five antifungal agents against dermatophytes, using the agar dilution and broth microdilution methods. Revista da Sociedade Brasileira de Medicina Tropical 42: 250–254.

Mendonça DE, Onofre SB (2009) Antimicrobial activity of the oil-resin produced by copaiba *Copaifera multijuga* Hayne (Leguminosae). Braz J Pharmacogn 19: 577–581.

Mengual O, Meunier G, Cayre I, Puech K, Snabre P (1999) TURBISCAN MA 2000: multiple light scattering measurements for concentrated emulsion and suspension instability analysis. Talanta 50: 445–456.

Moddaresi M, Brown MB, Zhao Y, Tamburic S, Jones SA (2010) The role of vehicle–nanoparticle interactions in topical drug delivery. Int J Pharm 400: 176–182.

Monod M (2008) Secreted proteases from dermatophytes. Mycopathologia 166: 285 – 294.

Muangman P, Aramwit P, Palapinyo S, Opasanon S, Chuangsuwanich A (2011) Efficacy of the combination of herbal extracts and a silicone derivative in the treatment of hypertrophic scar formation after burn injury. Afr J Pharm Pharmacol 5: 442–446.

Mukherjee PK, Leidich SD, Isham N, Leitner I, Ryder NS, Ghannoum MA (2003) Clinical Trichophyton rubrum strain exhibiting primary resistance to terbinafine. Antimicrob Agents Chemother 47: 82–86.

Müller RH, Mäder K, Gohla S (2000) Solid lipid nanoparticles (SLN) for controlled drug delivery - a review of the state of the art. Eur J Pharm Biopharm 50: 161–177.

Paiva LAF, Cunha KMA, Santos FA, Gramosa NV, Silveira ER, Rao VSN (2002) Investigation on the wound healing activity of oleo-resin from *Copaifera langsdorffii* in rats. Phytother Res 16: 737–739.

Park BJ, Taguchi H, Kamei K, Matsuzawa T, Hyon SH, Park JC (2011) *In vitro a*ntifungal activity of epigallocatechin 3-*O*-gallate against clinical isolates of Dermatophytes. Yonsei Med J 52: 535–538.

Peres NTA, Maranhão FCA, Rossi A, Martinez-Rossi NM (2010) Dermatophytes: host-pathogen interaction and antifungal resistance. Anais Brasil Dermatol 85: 657–667.

Perrot S, Dutertre-Catella H, Martin C, Warnet J-M, Rat P (2003) A new nondestructive cytometric assay based on resazurin metabolism and an organ culture model for the assessment of corneal viability. Cytometry Part A 55A: 7–14.

Pfaller MA, Diekema DJ (2004) Rare and emerging opportunistic fungal pathogens: concern for resistance beyond *Candida albicans* and *Aspergillus fumigatus*. J Clin Microbiol 42: 4419–4431.

Pieri FA, José RM, Galvão NN, Nero LA, Scatamburlo Moreira MA (2010) Antimicrobial activity of autoclaved and non-autoclaved copaiba oil on Listeria monocytogenes. Ciência Rural, Santa Maria 40: 1797–1801.

Prucek R, Tuček J, Kilianová M, Panáček A, Kvítek L, Filip J, Kolář M, Tománková K, Zbořil R (2011) The targeted antibacterial and antifungal properties of magnetic nanocomposite of iron oxide and silver nanoparticles. Biomaterials 32: 4704–4713.

Qian C, McClements DJ (2011) Formation of nanoemulsions stabilized by model food-grade emulsifiers using high-pressure homogenization: Factors affecting particle size. Food Hydrocolloids 25:1000–1008.

Qin L, Rutian L, Zhenshu Z, Xiaoping Q, Wenxian G, Lixia Y, Mi Y, Xiqun J, Baorui L (2012) Enhanced antitumor efficacy, biodistribution and penetration of docetaxel-loaded biodegradable nanoparticles. Int J Pharm 430: 350–358.

Sagrera G, Bertucci A, Vazquez A, Seoane G (2011) Synthesis and antifungal activities of natural and synthetic bioflavonoids. Bioorg Med Chem 19: 3060–3073.

Schaffazick SR, Guterres SS (2003) Caracterização e Estabilidade Físico-Química de Sistemas Poliméricos Nanoparticulados para Administração de Fármacos. Química Nova 26: 726–737.

Singh SB, Li X, Chen T (2011) Biotransformation of antifungal ilicicolin H. Tetrahedron Lett 52: 6190–6191.

Sokovic M, Van Griensven LJLD (2006) Antimicrobial activity of essential oils and their components against the three major pathogens of the cultivated button mushroom, Agaricusbisporus. Eur J Plant Pathol 116: 211–224.

Sznitowska M, Janicki S, Baczek A (2001) Studies on the effect of pH on the lipoidal route of penetration across stratum corneum. J Control Release 76: 327–335.

Thune P, Nilsen T, Hanstad I.K, Gustavsen T, Lovig Dahl H (1988) The water barrier function of the skin in relation to water content of stratum corneum, pH and skin lipids, Acta Derm.-Venereol 68: 277–283.

Vasconcelos KRF, Da Veiga Junior VF, Rocha WC, Bandeira MFCL (2008) *In vitro* assessment of antibacterial activity of a dental cement constituted of a *Copaifera multijuga* Hayne oil-resin. Braz J Pharmacogn 18: 733–738.

Veiga Junior VF, Rosas EC, Carvalho MV, Henriques MGMO, Pinto AC (2007) Chemical composition and anti-inflammatory activity of copaiba oils from *Copaifera cearensis* Huber ex Ducke, *Copaifera reticulata* Ducke and *Copaifera multijuga* Hayne - A comparative study. J Ethnopharmacol 112: 248–254.

Veraldi S, Menter A, Innocenti M (2008) Treatment of mild to moderate seborrhoeic dermatitis with MAS064D (Sebclair), a novel topical medical device: results of a pilot, randomized, double-blind, controlled trial. J Eur Acad Dermatol Venerol 22: 290–296.

Vermount S, Tabart J, Baldo A, Mathy A, Losson B, Mignon B (2008) Pathogenesis of dermatophytosis. Mycopathologia 166: 267–275.

Ying S, Chunyang L (2012) Correlation between phospholipase of *Candida albicans* and resistance to fluconazole. Mycoses 55: 50–55.

Zhao Z, Wang Q, Wang K, Brian K, Liu C, Gu Y (2010) Study of the antifungal activity of Bacillus vallismortis ZZ185 in vitro and identification of its antifungal components. Biores Technol 101: 292–297.

Zidan AS, Rahman Z, Khan MA (2011) Product and process understanding of a novel pediatric anti-HIV tenofovir niosomes with a high-pressure homogenizer. Eur J Pharm Sci 44: 93–102.